Fuel 374 (2024) 132502

Contents lists available at ScienceDirect

Fuel

journal homepage: www.elsevier.com/locate/fuel

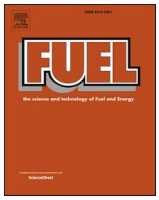

Full Length Article

Comprehensive study of valorisation of exhausted olive pomace through the preparation of highly porous activated carbons

H. Martínez-Alvarenga [a], M.C. Gutiérrez [a,b], A. Benítez [a,*], M.A. Martín [a,b,*], A. Caballero [a]

[a] Dpto. Química Inorgánica e Ingeniería Química, Instituto Químico para la Energía y el Medioambiente (IQUEMA), Universidad de Córdoba, 14014 Córdoba, Spain
[b] Campus de Excelencia Internacional Agroalimentario ceiA3, Universidad de Córdoba, Campus Universitario de Rabanales, N-IV, km 396, Córdoba 14071, Spain

ARTICLE INFO

Keywords:
Activated carbon
Alpeorujo
Olive
Thermochemical treatment
Valorisation

ABSTRACT

Exhausted olive pomace (EOP), commonly known as *alpeorujo*, is a by-product of olive oil production. EOP is recognised for the environmental risk associated with its current management and/or valorisation methods. This work aims to recover this agro-industrial waste through its conversion into functional activated carbon (AC). To achieve a successful transformation, a simple three-stage process was studied: (i) mechanical pre-activation by preparing four different proportions of *alpeorujo* with KOH as an activating agent (1:1, 2:1, 3:1, and 4:1); (ii) thermochemical treatment at different pyrolysis temperatures (600–1000 °C); and (iii) chemical purification. The overall process yield varies between 2–15 % depending on the selected conditions.

Innovatively, the liquid and gaseous effluents were characterised to propose an adequate valorisation approach. Additionally, mass, energy, and economic balances were carried out to analyse the profitability of the AC production process.

ACs with a very large specific area (>1600 m^2/g) and high carbon content (>90 %) were produced. The analysis of gaseous emissions from the thermochemical treatment resulted in a total yield of volatile organic compounds (VOCs) and volatile sulphur compounds (VSCs) of 874 and 2605 $mg/kg_{Alpeorujo}$, respectively, which is a disadvantage from an environmental perspective. The elements removed during the purification process achieved a total of 217.97 mg/g_{AC}, confirming the effectiveness of this stage. Finally, the cost of the *alpeorujo*-derived AC was estimated to be lower than €10/kg according to an economic analysis.

As a novelty, this work demonstrates that highly porous AC of this type can be obtained without the usual impregnation and pre-carbonisation steps using ultra-low proportions of a dry activating agent.

1. Introduction

Among agro-industrial processes, olive oil production generates notably large amounts of organic waste as a result of intensive agricultural practices [47]). Worldwide, Europe is the largest producer, exporter, and consumer of olive oil (66 % of global consumption). In terms of production, Italy, Greece, and Spain produce almost all the olive oil in the European Union (EU), approximately 2 million tons (94.23 % of EU olive oil production in the period 2015–2020). Spain accounts for 63.14 % of the EU production [27]. The valorisation of organic waste generated from various sources, such as municipal waste treatment plants and the agro-industrial and food sectors, is an alternative that has attracted significant research interest in order to obtain high-value products [45]. In fact, the European Commission has included this line of research and development in the EU's Circular Economy Action Plan; one of the cornerstones of the European Green

Abbreviations: **ACs**, activated carbons; **amu**, atomic mass units; **DMDS**, dimethyl disulphide; **DMS**, dimethyl sulphide; **EDS**, energy-dispersive X-ray spectrometry; **EOP**, exhausted olive pomace; **Ethyl-SH**, ethanethiol; **FS**, fixed solids (mg/kg, %); **FT-IR**, Fourier Transform Infrared; **IC**, soluble inorganic carbon (mg/kg); **N-NH_4^+**, ammoniacal nitrogen (mg/kg); **Methyl-SH**, methanethiol; **N-TKN**, total Kjeldahl nitrogen (mg/kg); **OD_{20}**, cumulative oxygen demand at 20h (mg O_2/g VS); **OP**, olive pomace; **ORR**, Oxygen Reduction Reaction; **P-P_2O_5**, phosphorous content (mg/kg); **S_{BET}**, specific surface area (m^2/g); **SEM**, scanning electron microscopy; **S_{micro}**, micropore area (m^2/g); **$SOUR_{max}$**, maximum specific oxygen uptake rate (mg O_2/g VS h); **STP**, standard temperature and pressure; **TC**, soluble total carbon (mg/kg); **TGA**, thermogravimetric analysis; **TN**, soluble total nitrogen (mg/kg); **TOC**, soluble total organic carbon (mg/kg); **V_{micro}**, micropore volume (cm^3/g); **VOCs**, volatile organic compounds; **VS**, volatile solids (mg/kg, %); **VSCs**, volatile sulphur compounds; **V_T**, total pore volume (cm^3/g).

* Corresponding authors at: Dpto. Química Inorgánica e Ingeniería Química, Instituto Químico para la Energía y el Medioambiente (IQUEMA), Universidad de Córdoba, 14014 Córdoba, Spain (M.A. Martin).

E-mail addresses: q62betoa@uco.es (A. Benítez), iq2masam@uco.es (M.A. Martín).

https://doi.org/10.1016/j.fuel.2024.132502
Received 11 March 2024; Received in revised form 5 July 2024; Accepted 11 July 2024
Available online 17 July 2024

Deal, Europe's new roadmap to achieve sustainable growth (European Commission, 2020).

Olive oil is obtained from a process of grinding and centrifuging the olives. This extraction generates a large amount of oil-impregnated waste [44]. For this reason, hexane, an organic solvent approved for food purposes, has been deployed to recover the oil and obtain pomace oil. Centrifugation is then repeated and, finally, the solution with hexane is distilled. The waste generated at the end of all the extractions is referred to as exhausted olive pomace (EOP), what is commonly known as *alpeorujo* or *alperujo*.

Alpeorujo could potentially be utilised in biotechnological processes. The pomace is composed mainly of high amounts of extractives and pectin, both of which are normally discarded and not used in the raw material valorisation process [43]. During olive oil production, a large amount of *alpeorujo* is produced, around 80 kg of *alpeorujo* per 20 kg of olive oil [13]. Currently, olive mill wastes are a significant source of environmental pollution as they contain large amounts of organic matter, among them phenols. Moreover, they contain phytotoxic and antimicrobial substances that could kill plants or reduce their growth under non-adequate concentrations [14]. For this reason, the valorisation of these wastes through their transformation into high-quality products is gaining relevance. In this line, the literature proposes a wide variety of valorisation methodologies with different advantages and drawbacks. Among the biological methodologies, Michailides et al. [41] reported that the co-composting of olive leaves and olive pomace (OP) is an interesting methodology that allows obtaining a proper manure to minimise the use of synthetic fertiliser, whose cost has been increasing in recent years. The final product proved to be a high-quality amendment with C/N 27.1 and high nutrient concentrations (N: 1.79 %, P: 0.17 %, K: 4.97 %, Na: 2.8 %). The application of compost obtained from four different olive mill wastes for two types of soil have been evaluated by other authors [12] and shown to have a minimum potential impact on groundwater quality. Gómez-Cruz et al. [30] fractionated *alpeorujo* into valuable components for valorisation: an aqueous extract rich in hydroxytyrosol and mannitol, lignins with antioxidant properties, and fermentable sugars. Another attractive alternative is anaerobic digestion to obtain energy from biogas. Batuecas et al. [10] compared the environmental impacts of two treatments: anaerobic digestion of olive oil production waste to produce energy from biogas or the direct release of the waste onto soil without any treatment. The authors demonstrated that anaerobic digestion could be a feasible alternative for olive mills to produce biogas from common olive oil wastes, thus reducing the environmental impact and adding value to the olive oil production chain [11].

As a thermophysical method, the valorisation of olive waste as biochar is also an interesting option due to the numerous advantages and applications of this material, among them as an adsorbent to remove polyphenols from olive mill wastewater [1]; as amendment in agriculture soils to evaluate the impact on soil properties, enzymatic activities, and/or crop growth [22]; or as a bulking agent to improve N cycling during manure composting [38].

For olive solid waste, the physico-chemical preparation of ACs has been proposed for the efficient transformation of *alpeorujo*. Furthermore, unlike biochar, ACs present a high specific surface area, which allows them to be widely used in liquid and gas adsorption treatments and/or in energy storage systems. This is due to their effective and competitive cost, especially when the ACs are obtained from biomass waste [28].

However, few studies have reported on obtaining AC from *alpeorujo*. which, to the best of our knowledge, has been previously described in only four studies. Elmouwahidi et al. [26], for example, proposed obtaining advanced carbon materials (carbon content > 90 %; surface area of 1626 m^2/g) from the solid waste of wastewater used in the olive oil industry. AC was tested as electro-catalysts for the oxygen reduction reaction (ORR) in a three-electrode electrochemical set-up. A year later, the same author obtained AC derived from *alpeorujo* activated with KOH and H_3PO_4 by different processes to be used as supercapacitor electrodes. The ACs were obtained with specific surface values (above 771 m^2/g) appropriate for their application [25]. Ayadi et al. [9] proposed the preparation of a heterogeneous catalyst from OP to obtain biodiesel. The resulting AC presented a highly developed micropore structure and remarkable surface area (>600 m^2/g), making it useful as a catalyst of the esterification process. Finally, Şirazi and Aslan [50] also used OP as a precursor to obtain AC using KOH as an activating agent. The authors obtained ACs with a specific surface area (S_{BET}) from 386 m^2/g to 2452 m^2/g. In general terms, these four research studies prepared biocarbon endowed with outstanding physico-chemical and textural properties. However, different AC synthesis methods require complex processes with multiple stages. In some cases, they performed a pre-carbonisation stage, increasing the energy consumption. In other cases, the chemical activation was carried out by impregnation, which is much more complex than direct activation. These conditions are unfavourable for scaling at an industrial level. Moreover, high proportions of activating agents were used in all these studies, increasing the cost and overconsumption of resources. Furthermore, most of these works do not address the evaluation of the process globally, including co-products and generated waste. These weaknesses were also detected in most of the recent advances reported in the extensive and local production of ACs derived from agro-industrial wastes, as evidenced in studies on biodegradable materials such as banana peel [51], bamboo[21], or fruit wastes [33], among other materials.

This study is pioneering in that it provides an integral and simple AC synthesis process from *alpeorujo* with a potential for scaling up. Specifically, the gaseous and liquid waste generated during the process to obtain AC is analysed for treatment or valorisation. To estimate the economic viability of the AC generation process, including the drying and pyrolysis of the raw material (at laboratory scale), economic, mass, and energy balances are made. As a notable novelty, this work demonstrates the possibility of obtaining highly porous AC derived from *alpeorujo* using a synthesis process that does not require the impregnation and pre-carbonisation steps. This drastically reduces the amount of activating agent required and eliminates the need to add water to produce porosity in the carbonaceous product.

2. Materials and methods

2.1. Raw material characterisation: Alpeorujo

The *alpeorujo* studied in this research was supplied by the Andalusian cooperative Ntra. Sra. de la Consolación (Doña Mencía, Spain). The *alpeorujo* was produced during the 2021/2022 olive harvest. Since the waste was granular and had a high moisture content, the sample was dried at 65 °C in the laboratory and then subjected to a manual grinding process to obtain a homogeneous sample.

Once a dry and homogeneous *alpeorujo* was achieved, it was physico-chemically analysed following the Test Methods for the Examination of Compost and Composting of the US Department of Agriculture and Composting Council TMECC, Test Methods for the Examination of Compost and Composting, [55] (see Supplementary Material: Text 1).

Finally, thermogravimetric analyses were performed in a TGA/DSC-1 Star System Mettler-Toledo thermobalance by heating the samples in 100 μL alumina crucibles from room temperature to 900 °C at a rate of 10 °C/min under a 100 mL/min flow rate of an oxygen or nitrogen atmosphere depending on the analysis required.

In addition, the elements contained in the *alpeorujo* ashes, obtained after the carbonisation of the raw material at 550 °C, were determined by X-ray fluorescence measurements. The spectra were acquired with a Rigaku wavelength dispersive X-ray fluorescence (WDXRF) spectrometer, ZSX Primus IV. Additionally, scanning electron microscopy (SEM) images of the ashes were obtained with a JEOL JSM-7800F scanning electron microscope equipped with an X–ACT (Cambridge Instrument) detector for energy-dispersive X-ray spectrometry (EDS) elemental

microanalysis. An acceleration voltage of 5.0 KV was used to obtain qualitative information on the composition of the samples.

All the variables mentioned above were analysed in triplicate and the mean values and standard deviations were obtained for each one.

2.2. AC preparation process

To convert the *alpeorujo* into AC, three sequential stages were performed: (i) mechanical pre-activation; (ii) thermochemical treatment; and (iii) chemical purification. Scheme 1 shows the stages of the chemical activation method. The preparation of ACs by KOH requires two steps: i) activation of the raw precursor material with KOH solution followed by ii) carbonisation at high temperature or vice versa [32]. To optimise the preparation process for industrial scale-up, the number of activation steps can be reduced by replacing the KOH solution with solid KOH. Therefore, in the present work, a direct KOH-activation step was performed to synthesise AC with *alpeorujo* as the precursor material.

(i) Mechanical pre-activation

Potassium hydroxide (KOH, Panreac, 85 %) in solid form was used as the chemical activating agent. Moreover, the effect of the amount of activating agent was evaluated by preparing four different *alpeorujos*: KOH mass ratios (1:1, 2:1, 3:1, and 4:1). Both components were mixed using an agate mortar until a completely homogeneous composite was obtained.

(ii) Thermochemical treatment

The thermochemical treatment was performed by pyrolysis in an inert atmosphere. The mixture was placed in a ceramic crucible and introduced into a tube furnace under continuous nitrogen gas flow (50 mL/min_{STP}), where the pyrolysis was developed to obtain an AC. To study the effect of the activation temperature, the calcination stage was carried out by setting different target temperatures (600, 700, 800, 900, and 1000 °C) at a heating rate of 10 °C/min. Once the target temperature was reached, it was kept constant for 1 h. The system then started cooling down, maintaining a constant flow of nitrogen gas. The thermochemical treatment yield ($\eta_{Pyrolysis}$, %) was calculated using the following equation (Eq. (1)):

$$\eta_{Pyrolysis}(\%) = \frac{m_1}{m_0} \bullet 100 \quad (1)$$

where m_0 (g) is the *alpeorujo* weight mixed with KOH to be pyrolysed, and m_1 (g) is the AC mass obtained after the thermochemical treatment.

(iii) Chemical purification

The aim of this stage is to remove all types of impurities in the AC. A 6 M hydrochloric acid solution was used for the chemical purification treatment (HCl, Panreac, 37 %). In an Erlenmeyer flask, 40 mL of 6 M HCl solution was added for each gram of AC obtained, ensuring complete impregnation. The suspension was then shaken at 175 rpm for 90 min using an orbital shaker. Subsequently, the sample was microfiltered through a 47 mm Whatman glass fibre filter and washed with approximately 3 to 5 L of distilled water until the wash water reached a neutral pH. Finally, the AC was introduced into an oven at 105 °C for 24 h to remove the moisture and obtain the final product, a solid black mass with a powdery texture.

The chemical purification yield ($\eta_{Purification}$, %) was calculated using the following equation (Eq. (2)):

$$\eta_{Purification}(\%) = \frac{m_2}{m_1} \bullet 100 \quad (2)$$

Where m_1 (g) is the AC mass obtained after the thermochemical treatment and m_2 (g) is the AC mass obtained after the chemical purification treatment.

The overall yield of the process (η_{Total}, %) was calculated by using Eq. (3):

$$\eta_{Total}(\%) = \frac{\eta_{Pyrolysis}(\%) \bullet \eta_{Purification}(\%)}{100} \quad (3)$$

where $\eta_{Pyrolysis}(\%)$ and $\eta_{Purification}(\%)$ were previously defined in the Eq. (1) and Eq. (2), respectively.

To ensure an adequate amount of material for all the analytical determinations, a minimum of 5 replicates were performed, unifying the resulting product.

The ACs were denoted as AK where "A" stands for *alpeorujo* and "K" for KOH. The following AKs were obtained: AK_11_600, AK_21_600, AK_31_600, AK_41_600, AK_21_700, AK_21_800, AK_21_900, and AK_21_1000; followed by the A:K mass ratio (1:1, 2:1, 3:1 or 4:1) where the first digit corresponds to *alpeorujo* and the second to KOH. Finally, the activation temperature (600, 700, 800, 900, or 1000 °C) was also included in the nomenclature.

2.3. Characterisation of the ACs obtained after the process to transform the alpeorujo

A complete characterisation of the *alpeorujo*-derived ACs was carried out to determine their composition, moisture, carbon, and nitrogen content, as well as their thermal behaviour and textural properties.

In accordance with the methodology described in the Test Methods for the Examination of Compost and Composting TMECC, Test Methods for the Examination of Compost and Composting, [55] for the characterisation of raw materials, the following variables were determined for the ACs. FS (%) and VS (%) were analysed in the solid fraction. All variables were determined in triplicate, showing the mean values and standard deviation. In addition, the proportions of moisture, carbon content, and mineral matter were analysed by thermogravimetric analysis (TGA). The elemental analysis was carried out in a LECO CNS-928 macro-analyser. The porosity of the ACs was characterised by N_2 adsorption–desorption at −196 °C (77 K) using a Micromeritics ASAP 2020 M. The ACs were dried at 90 °C for 1 h, followed by outgassing at 150 °C for 4 h prior to being tested. From the N_2 adsorption isotherm,

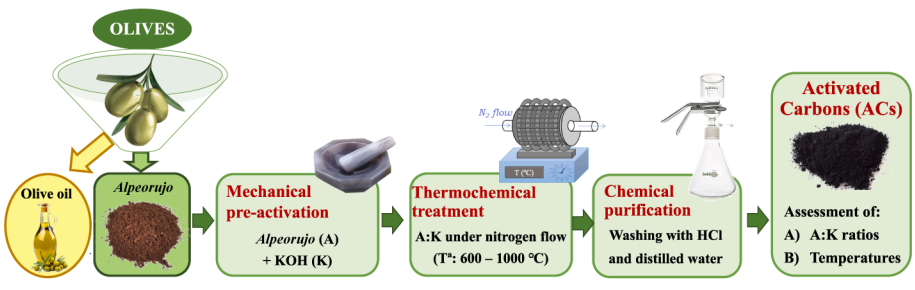

Scheme 1. Diagram of stages to obtain ACs.

the S_{BET} was determined by applying the Brunauer–Emmett–Teller (BET) equation when the range of relative pressures was from 0.04 to 0.20. The total pore volume (V_T) was calculated at a relative pressure of $P/P_0 = 0.98$. The pore size distribution was evaluated using the density functional theory (DFT). The *t*-plot method was applied to calculate the micropore area (S_{micro}) and micropore volume (V_{micro}).

In order to identify the existing functional groups in the AC, Fourier Transform Infrared (FT-IR) spectrum analyses were conducted in the 4000–400 cm^{-1} region using transmission mode with a PerkinElmer Frontier instrument.

Additionally, to determine the surface charge of the AC, zeta potential measurements were carried out using laser Doppler velocimetry with a ZetasizerNano ZS (Malvern Panalytical, Malvern, UK) in aqueous solution. The solution pH was adjusted to the required pH in the range of 1–10 using 0.1 M of HNO_3 or KOH.

2.4. Evaluation of the gaseous and liquid effluents produced during the transformation of alpeorujo into AC

An in-depth study of the process was conducted by analysing the different streams generated in both the thermochemical treatment and the purification stage.

The gaseous products generated during the thermochemical treatment were characterised using gas chromatography coupled with mass spectrometry (GC/MS) combined with an analyser capable of tracking the total concentration of volatile organic compounds (VOCs) and some volatile sulphur compounds (VSCs). Finally, the content of elements in the liquid effluents and the composition of the wash water generated during the chemical purification stage were evaluated using X-ray fluorescence.

2.4.1. Study of the condensable and non-condensable fraction generated during thermochemical treatment

The non-condensable gaseous stream derived from the thermochemical treatment was characterised by two types of experiments with the objective of performing (i) a continuous analysis to evaluate all gases generated during the whole process and (ii) a discontinuous analysis with the purpose of knowing the concentration of gases emitted every 10 min of the process.

For this purpose, the gases generated during the thermochemical treatment passed through a gas trap to a cooling chamber (Julabo F250). This allowed us to obtain a condensable and a non-condensable fraction and characterise each one.

A continuous analysis of the non-condensable gases was carried out. The gas stream was collected in an 8 L Nalophan® bag followed by concentration on a sorbent tube filled with Tenax® Porous Polymer Adsorbent and Carbograph 5TD, in 1:1 proportion (w/w), with a sampling pump (Markes Easy-VOC) (Experimental conditions were described in Supplementary Material: Text 2).

A discontinuous analysis was also performed to determine the non-condensable gaseous compounds generated at each moment of the thermochemical treatment. To do this, 1L Nalophan® bags were filled every 10 min following the same process described above. These bags were immediately analysed in a specific chromatograph (Chromatotec Vigi e-nose M52022) to determine the concentration of VOCs (mg/m^3) and VSCs (mg/m^3) as sulphur spectra, including methanethiol (methyl-SH), hydrogen sulphide (H_2S), dimethyl disulphide (DMDS), and ethanethiol (ethyl-SH).

The following conversion equation was used to determine the yield of the gaseous products, taking into account that the instrumentation provides the concentration values in mg/m^3. Continuous material balances of the non-stationary process were carried out to obtain the VOC and VSC point yields and total pyrolysis yield according to Eq. (4):

$$\frac{mg_{VOC,VSC}}{kg_{Alpeorujo}} = \frac{[VOC, VSC]\left(\frac{mg}{m^3}\right) \bullet Q\left(\frac{m^3}{s}\right) \bullet t(s)}{m_{Alpeorujo}(kg)} \quad (4)$$

where [VOC, VSC] is the concentration of VOC or VSC provided by the equipment (mg/m^3), Q is the flow (m^3/s), t is the time of the experiment (s), and $m_{Alpeorujo}$ is the mass of the *alpeorujo* (kg).

For purposes of further study, the condensed fraction was also analysed. First, an elemental analysis was performed using a LECO CHNS-932 microanalyser. The higher heating value (HHV) was determined using a Parr 6300 calorimeter. A GC/MS (Bruker Mod Scion) was then used to identify the main compounds. For this purpose, the sample was subjected to liquid–liquid microextraction with ethyl acetate, with vortex agitation for 15 min. The sample was then centrifuged and a 1 mL aliquot was taken to which a small amount of ethyl sulphate was added. Finally, the extract was analysed by GC/MS at the Central Research Support Service of the University of Cordoba.

2.4.2. Analysis of elements in the chemical purification liquid and wash water

The chemical elements contained in the effluents generated during the acid purification and subsequent washing process were analysed in triplicate by X-ray fluorescence. Once the results were obtained, the concentrations of elements per gram of product were determined by Eqs. (5) and (6).

$$[E]_{purification}\left(\frac{mg_E}{g_{product}}\right) = \sum_{i=1}^{n} \frac{[E_i]\left(\frac{mg}{L}\right) \bullet V_{HCl}(L)}{m_{product}(g)} \quad (5)$$

$$[E]_{washing}\left(\frac{mg_E}{g_{product}}\right) = \sum_{i=1}^{n} \frac{[E_i]\left(\frac{mg}{L}\right) V_{H_2O}(L)}{m_{product}(g)} \quad (6)$$

where $[E]_{purification}$ and $[E]_{washing}$ are the concentration of elements present in the purification and washing effluents, respectively; *n* refers to each of the elements detected (P, Ca, Mg, S, Al, Fe, Na, and Ni); V_{HCl} and V_{H_2O} are the volumes of HCl and H_2O used during the chemical purification and washing stages, respectively; and $m_{product}$ is the final mass obtained from AC after the entire transformation process.

The percentage of elements removed, considering the element content initially present in the raw material, was calculated by means of the following equation:

$$ElementsRemoved(\%) = \sum_{i=1}^{n} \frac{\left[[E_i]\left(\frac{mg}{L}\right) \bullet V_{HCl}(L) + [E_i]\left(\frac{mg}{L}\right) \bullet V_{H_2O}(L)\right]}{m_{Alpeorujo}(mg)} \text{Â·} 100 \quad (7)$$

Where $m_{Alpeorujo}$ is the amount of *alpeorujo* used for further transformation into AC.

Finally, the composition of the wash water was analysed following standard methods [7] to determine parameters such as pH, conductivity, and the concentration of chlorides, sulphates, total solids, and fixed solids.

3. Results and discussion

3.1. Raw material analysis

Table 1 shows the physico-chemical characterisation of the raw material, *alpeorujo*, from which the ACs were prepared. These results have been confirmed with data reported in previous studies of *alpeorujo* (Albuquerque et al., 2009).

As observed, *alpeorujo* presents a high moisture content (70 %), so a preliminary stage to dry the raw material is usually necessary. In

Table 1
Physico-chemical characterisation of the raw material (alpeorujo).

VARIABLES	Values	VARIABLES	Values
pH	5.97 ± 0.02	*K (mg/kg)*	41,800 ± 9670
Conductivity (μS/cm)	1926 ± 5	*Ca (mg/kg)*	10,900 ± 120
Moisture (%)	70.02 ± 0.02	*Si (mg/kg)*	4340 ± 26
TC (mg/kg)	147,829 ± 15	*Cl (mg/kg)*	4090 ± 224
IC (mg/kg)	237 ± 5	*Mg (mg/kg)*	3640 ± 340
TOC (mg/kg)	147,592 ± 7	*S (mg/kg)*	2090 ± 580
TN (mg/kg)	2175 ± 10	*Al (mg/kg)*	1320 ± 254
FS (mg/kg)	67,621 ± 1740	*Fe (mg/kg)*	721 ± 12
VS (mg/kg)	932,379 ± 2000	*Na (mg/kg)*	241 ± 18
N-NH_4^+ (mg/kg)	1011 ± 30	*Zn (mg/kg)*	58.8 ± 2.5
N-TKN (mg/kg)	9816 ± 340	*Cu (mg/kg)*	47.2 ± 1.9
P-P_2O_5 (mg/kg)	2946 ± 10	*Ni (mg/kg)*	38.7 ± 1.6
$SOUR_{MAX}$ (mg O_2/g VS·h)	50.56 ± 2.00	*Sr (mg/kg)*	22.20 ± 0.02
OD_{20} (mg O_2/g VS)	215 ± 5	*Rb (mg/kg)*	17.70 ± 0.03

addition, this by-product showed a slightly acidic pH, which could make its biological valorisation through composting processes [5]or anaerobic digestion difficult [46]. Consequently, although *alpeorujo* is an organic waste with high potential for use as an organic amendment, it must be composted with other waste to balance the negative variables it presents.

Alpeorujo also contains carbon, nitrogen, and phosphorus. The values of these elements are shown in Table 1 through the following variables: TC (mg/kg), IC (mg/kg), TOC (mg/kg), TN (mg/kg), N-NH_4^+ (mg/kg), N-TKN (mg/kg), and P-P_2O_5 (mg/kg). These variables are of greater interest when *alpeorujo* is valorised for biological processes [57]. Even so, it is of interest to determine the nitrogen and phosphorus content because some studies have confirmed that the presence of heteroatoms such as N and P is beneficial in the structure of carbonaceous materials [4]. The VS, which are indicative of the total organic matter content, were high (93 %), in line with the content reported in other studies [58]. This finding suggests that a feasible solution to valorise this waste would be its transformation into biochar or AC since the main interest is to obtain a solid carbonaceous product [29]. The quantity of FS indicates the presence of mineral matter in the raw material (*alpeorujo*). This proportion was around 7 %, lower than what has been reported in the literature [48].

Until now, high volumes of *alpeorujo* have been stored in rafts outdoors. In addition to bad odours, the natural degradation of this waste produces emissions that contribute to the increase in greenhouse gases [3]. The microbiological activity and biodegradability of *alpeorujo* were determined as $SOUR_{MAX}$ (mg O_2/g VS·h), and OD_{20} (mg O_2/g VS), respectively. The $SOUR_{MAX}$ value was appropriate for treatment in a biological process and natural fermentation in storage ponds, which produces malodorous gaseous emissions. The values obtained differed greatly from those that indicate microbiological stability ($SOUR_{MAX} < 1$ mg O_2/g VS·h). The OD_{20} result reflected a moderately high biodegradability. These parameters have been used previously to evaluate the microbiological stability and biodegradability of sewage sludge [40], but have also been used in other agricultural wastes such as *alpeorujo*, showing results similar to those obtained [56].

In addition, a remarkable variety of elements were presented in the raw material as determined by X-ray fluorescence measurements of the *alpeorujo*-derived ashes (Table 1). Their presence was also confirmed through SEM/EDS mapping. In Fig. S1a, an SEM image of the *alpeorujo* ashes shows a poorly defined morphology constituted by agglomerates. Moreover, the compositional distribution of the ashes is shown in Fig. S1b with mainly K, O, C, Ca, Mg, P, Cl, Si, S, Al, and Fe detected. The elements found in the highest proportion in the ashes at the surface level were correlated with those analysed by WDXRF as shown in Table 1.

Fig. 1 shows the thermal behaviour of the *alpeorujo* on a dry basis by TGA measurements under oxidising and inert atmospheres. In both cases, the first region was at a temperature below 90 °C where there was a slight decrease in weight due to the presence of surface moisture. In the

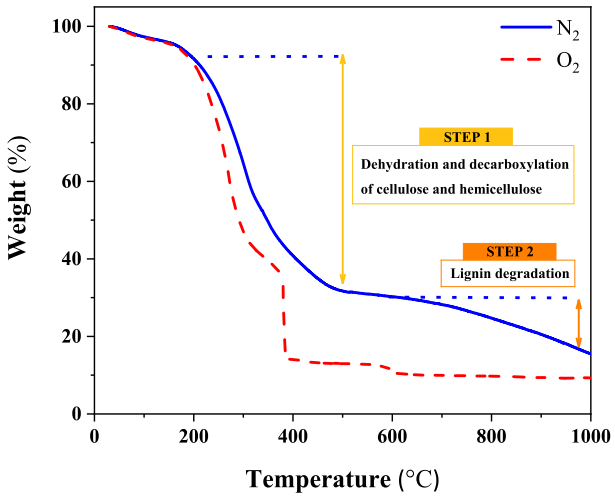

Fig. 1. TGA of raw material on a dry basis under O_2 and N_2 flow.

TGA under an oxygen atmosphere (dot plot), a loss of weight was observed at temperatures between 200 °C and 500 °C. This was due to the combustion of the organic matter, which corresponded to 90 % of the weight. After combustion, the remaining weight corresponded to mineral matter. Regarding the TGA under a nitrogen atmosphere (line plot), the main transformation of the organic matter into carbon occurred at temperatures close to 550 °C. For this reason, the temperatures selected to transform *alpeorujo* into AC were set above 600 °C in this work. The transformation of *alpeorujo* into AC involves a series of successive stages [9]. At the first stage of reaction, dehydration and decarboxylation of cellulose and hemicellulose cause the release of CO and CO_2 between 230 °C and 500 °C. Up to 600 °C, lignin degradation is produced, generating mainly CH_4. At high temperature levels, H_2 can be released.

3.2. Effect of alpeorujo and KOH mass ratio on AC properties

As described in Materials and Methods, the ACs were pyrolyzed using four mass ratios of *alpeorujo* and KOH (A:K = 1:1, 2:1, 3:1, 4:1) to evaluate the influence of the activating agent on the textural and chemical properties. In a novel manner, unlike the usual trend in previous publications on direct chemical activation (where the KOH weight is always greater than the precursor weight) [24], this work investigated the use of low proportions of activating agent in order to reduce three key topics: consumption of resources, environmental hazards, and cost of the final product. Table 2 presents the results of the physico-chemical and thermogravimetric characterisation as well as the nitrogen content determined from the elemental analysis. No significant differences were observed regarding the physico-chemical characteristics acquired by the prepared ACs. However, there was a slight increasing trend of both VS and nitrogen content due to the progressive increase in the amount of *alpeorujo* with respect to the activating agent. Even so, these differences did not exceed 1 %. The presence of nitrogen in the ACs may be relevant in applications such as catalysis, energy storage, adsorption, etc. [37].

TGA curves of ACs synthesised at 600 °C using different activation ratios showed a similar profile (Fig. S2). All the ACs provided a percentage of carbon above 8 %. The main stage of weight loss was observed at around 400 °C. This may be due to the combustion of carbon, the major component in ACs. Likewise, the weight loss below 100 °C allowed the moisture content in the samples to be quantified, which reached maximum values of 13 % in all cases.

In addition, nitrogen adsorption/desorption isotherm measurements were performed to evaluate the textural properties. According to the Brunauer, Deming, Deming, and Teller (BDDT) classification, the adsorption/desorption isotherms for ACs synthesised at different A:K

Table 2
Physico-chemical characterisation and textural properties of ACs prepared at an activation temperature of 600 ºC with different A:K mass ratios.

Physico-chemical characterisation					
Samples	**Physico-chemical charact.**		**Thermogravimetric charact.**		**Elemental** [2]
	FS (%)	*VS (%)*	*Moisture (%)*	*C (%)* [1]	*N (%)* [1]
AK_11_600	6.08 ± 0.03	93.92 ± 0.84	13	81	0.93
AK_21_600	7.27 ± 0.02	92.72 ± 3.60	8	92	0.95
AK_31_600	5.75 ± 0.79	94.25 ± 1.84	13	87	1.13
AK_41_600	5.06 ± 0.31	94.94 ± 0.22	7	87	1.10
Textural properties					
Samples	S_{BET} (m^2/g)	S_{micro} (m^2/g)	V_T (cm^3/g)	V_{micro} (cm^3/g)	***Microporosity*** [3] (%)
AK_11_600	786	644	0.429	0.316	74
AK_21_600	726	629	0.403	0.308	76
AK_31_600	625	542	0.353	0.266	75
AK_41_600	676	582	0.404	0.285	70

[1] Dry basis; [2] Elemental analysis; [3] Calculated by dividing V_{micro} and V_T and multiplying by 100; FS, fixed solids; VS, volatile solids; C, carbon content; N, nitrogen content; S_{BET}, specific surface area; S_{micro}, micropore area; V_{micro}, micropore volume; V_T, total pore volume.

mass ratios exhibited type I and IV profiles (Fig. 2a) with a hysteresis loop indicating the presence of mesopores. These isotherms are in line with those reported by Elmouwahidi et al. [25] which obtained ACs derived from olive residues. This combined behaviour corresponds to the typical curve of microporous solids (at low relative pressure P/P_0) and mesoporous solids (at intermediate relative pressures P/P_0), indicating a dual pore system. During the KOH activation process, surface species such as alkaloids and molecular species such as K_2CO_3, K_2O, and K are formed. The reactions that occurred during the chemical activation between KOH and the lignocellulosic material (*alpeorujo*) are described below [23]:

$$Ligno. + KOH \xrightarrow{\Delta} Ligno.K_2O + H_2O(liquid) \quad (8)$$

$$Ligno. + H_2O \xrightarrow{\Delta} Char, C + H_2O(gas) + Tar \quad (9)$$

$$C + H_2O(gas) \xrightarrow{\Delta} H_2 + CO \quad (10)$$

$$CO + H_2O(gas) \xrightarrow{\Delta} H_2 + CO_2 \quad (11)$$

$$K_2O + H_2 + CO_2 + Char, C \xrightarrow{\Delta} Char + K_2CO_3 + K \quad (12)$$

The well-defined porosity of *alpeorujo*-derived ACs is a result of activation with KOH and can be attributed to potassium interaction and the stretching of carbon layers. KOH is highly effective at creating micropores due to an interaction between layers [35].

Furthermore, Fig. 2b shows the pore size distributions as determined by density functional theory (DFT), which confirmed the presence of a certain proportion of micropores (below 2 nm) and macropores larger than 50 nm. Nevertheless, the results indicated that the primary adsorption sites for the adsorbate were in the mesopore range, distinguishing two regions, one around 10 nm and the other between 25 and 50 nm.

The values obtained for the textural parameters are also shown in Table 2. It should be noted that there was no significant variation in the data for S_{BET}, V, and microporosity (%) between the samples prepared at 600 °C with different A:K mass ratios. Therefore, the A:K mass ratio affects the textural properties but does not play a key role in porosity modelling. According to the data reported by Chayid and Ahmed [16], an increase in the amount of potassium expands the porosity and micro- and mesopores are formed in the off-centre walls of the pores, which increases the S_{BET} values. In addition, by increasing the dosage of potassium hydroxide, microporous pores develop on the surface of the AC (enhancing the microporosity %), while the mesoporous pores decrease due to the characteristics of the potassium hydroxide activators [60].

A comparison of these results with those reported by other authors revealed that ACs with higher S_{BET} and V_T values were sometimes

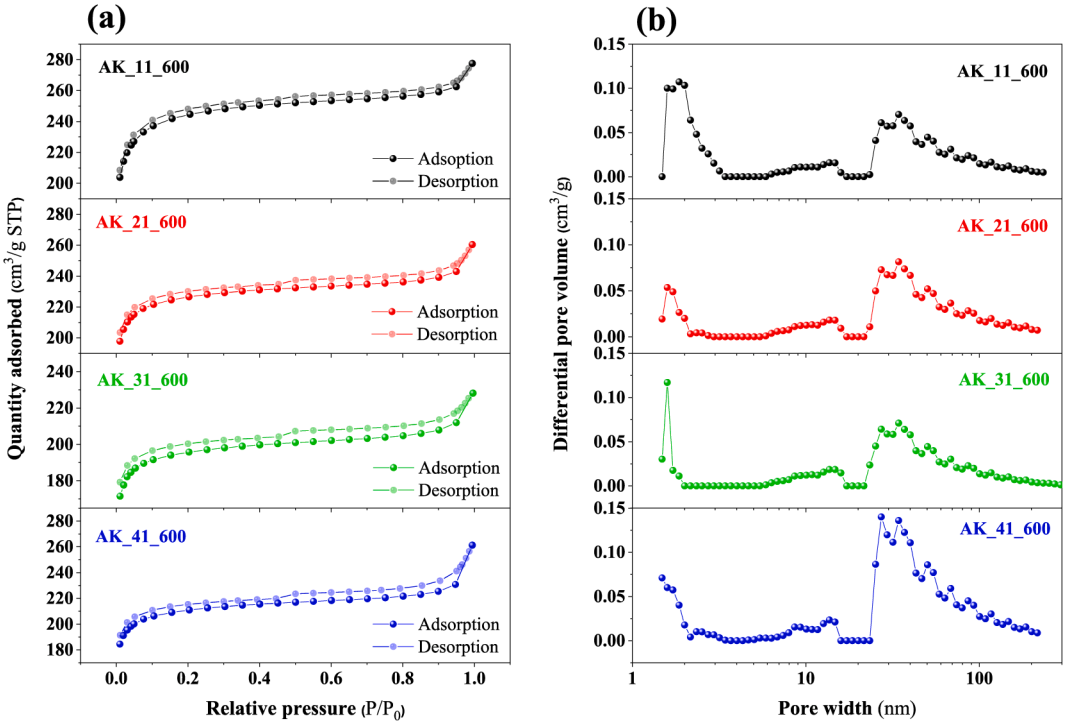

Fig. 2. (a) N_2 adsorption/desorption isotherms and **(b)** pore size distributions for ACs prepared at an activation temperature of 600 °C at different A:K mass ratios.

obtained through the transformation process carried out in this study [2]. In other cases, ACs with higher S_{BET} values were found due to the complexity and long duration of their processes, which allow an increase in the textural properties [19].

In order to evaluate the viability of the process to transform *alpeorujo* into ACs, the overall performance of the process was calculated. Table 3 shows the thermochemical treatment and chemical purification yields, as well as the overall yield for the ACs obtained at 600 °C with different A:K mass ratios. As can be observed, the yield of the thermochemical treatment increases with an increasing amount of KOH in the mixture. When four times less activating agent is used half the yield is obtained due to the loss of carbonaceous matter. Conversely, the chemical purification yields increased by 2 % since less of the activating agent (KOH) was used. As for the overall yield, a maximum value of 15 % was obtained in the sample with a 3:1 ratio, although no significant variation was observed between the overall yields of the different samples.

After analysing the results, the AK_21_600 sample was selected for further study. This sample corresponded to the AC at 600 °C with a 2:1 mass ratio of *alpeorujo* to KOH. The rationale behind this decision was the large surface area of this sample. While the surface area was only 8 % less than the AK_11_600 sample, the amount of activating agent was reduced by half. Specifically, the AK_21_600 sample exhibited a S_{BET} of 726 m^2/g, a V_T of 0.403 cm^3/g, and microporosity of 76 %. Moreover, this sample achieved a good overall process yield.

Once this AC was selected, a further study was conducted to determine the possible effects of a variation in pyrolysis temperature on the ACs prepared with an A:K ratio of 2:1.

3.3. Effect of temperature on AC properties

The effect of pyrolysis temperature was a key aspect to be evaluated in the preparation of ACs from by-products in order to identify the optimum conditions for the thermochemical treatment [6,59]. In this study, five different temperatures were selected (600, 700, 800, 900, and 1000 °C) and the 2:1 A:K ratio was maintained.

Table 4 shows that the composition of the synthesised ACs varied significantly when the temperature was modified, thus indicating that temperature has a clear influence on AC synthesis. Specifically, it was observed that the percentage of VS decreased at higher activation temperatures, except in the range of 600 to 700 °C where an increase of 5 % occurred. This effect is consistent with the findings of Lua and Yang [39], who reported that an increase in temperature resulted in the release of VS.

Fig. S3 shows the TGA curves recorded under oxygen flow for ACs synthesised at different temperatures. The results are shown in Table 4. The profiles were similar to those obtained for ACs synthesised at 600 °C using different A:K ratios (Fig. S2). In this case, the first weight loss was observed below 100 °C, which corresponds to the removal of moisture, which in all cases was less than 8 %. In addition, a more pronounced weight loss occurred around 400 °C, which has been associated with the combustion of carbon, leaving the percentage of mineral solids as waste. The results obtained from the TGA allowed calculating the carbon content of the pyrolysed samples at different temperatures, which exceeded 88 % in all ACs. Finally, as can be seen, the nitrogen content significantly decreased at 600 °C to 700 °C, but the rest of the samples maintained a similar nitrogen content of around 0.63 %.

Table 3
Performance of the activating process carried out at the activation temperature of 600 °C with different A:K mass ratios.

Samples	*Thermochemical treatment yield* (%)	*Chemical purification yield* (%)	*Overall yield* (%)
AK_11_600	61.74	11.69	7.22
AK_21_600	50.19	22.51	11.30
AK_31_600	46.36	31.90	14.79
AK_41_600	30.04	37.95	11.40

The standard deviation between replicates was less than 0.01 % in all cases.

Table 4
Physico-chemical characterisation and textural properties of ACs prepared at different pyrolysis temperatures.

Physico-chemical characterization

Samples	**Physico-chemical charact.**		**Thermogravimetric charact.**		**Elemental** [2]
	FS (%)	VS *(%)*	*Moisture (%)*	*C (%)* [1]	*N (%)* [1]
AK_21_600	7.27 ± 0.02	92.72 ± 3.60	8	92	0.95
AK_21_700	2.37 ± 0.13	97.63 ± 2.84	7	88	0.63
AK_21_800	2.55 ± 1.20	97.45 ± 2.24	7	93	0.60
AK_21_900	4.43 ± 3.35	95.57 ± 0.63	5	94	0.64
AK_21_1000	10.04 ± 0.00	89.96 ± 6.51	5	91	0.62

Textural properties

Samples	S_{BET} (m^2/g)	S_{micro} (m^2/g)	V_T (cm^3/g)	V_{micro} (cm^3/g)	*Microporosity* [3] (%)
AK_21_600	726	629	0.403	0.308	76
AK_21_700	845	554	0.470	0.274	58
AK_21_800	1408	1041	0.762	0.519	68
AK_21_900	1639	1071	0.929	0.536	58
AK_21_1000	1254	679	0.822	0.335	41

[1] Dry basis; [2] Elemental analysis; [3] Calculated by dividing V_{micro} and V_T and multiplying by 100; FS, fixed solids; VS, volatile solids; C, carbon content; N, nitrogen content; S_{BET}, specific surface area; S_{micro}, micropore area; V_{micro}, micropore volume; V_T, total pore volume.

As regards the textural properties, the N_2 adsorption–desorption isotherms presented in Fig. 3a show the results obtained for the ACs pyrolysed at different temperatures. All the curves were type I and IV isotherms in accordance with the IUPAC classification, thus indicating the presence of microporous carbons with considerable mesoporosity. In fact, the type IV isotherm is characterised by its hysteresis loop, which is associated with capillary condensation taking place in the mesopore area.

To clarify the type of pores in the samples, the pore size distributions determined by DFT are shown in Fig. 3b, confirming the presence of micropores as well as mesopores and macropores. Specifically, an increasing trend in the region of low mesoporosity (between 2–5 nm) was observed as the pyrolysis temperature increased. The reaction between the activating agent and the precursor of carbon materials results in the decomposition of VOCs, thus creating a highly porous surface in the AC samples.

The textural properties of the *alpeorujo*-derived ACs are reported in Table 4. The values of S_{BET}, V_T, and V_{micro} tended to increase as the temperature rose. However, the behaviour of the AK_21_1000 sample differed from the others. As reported in the literature, this is because the porous structure collapses at high temperatures and the textural properties worsen [53]. The number of pores may be reduced due to structural ordering or pore widening, while some pores may be blocked due to the softening, melting, and fusing of ash [17]. Therefore, the textural parameters decreased for temperatures above 900 °C. A decrease in the percentage of microporisity can also be observed when the pyrolysis temperature is increased. This is due to the widening of micropores to mesopores, as was previously reported when KOH is used as an activating agent in producing ACs from waste biomass [54]. The ultra-high values exhibited by the AK_21_900 sample are notable, with an S_{BET} of 1639 m^2/g, V_T of 0.929 cm^3/g, and V_{micro} of 0.536 cm^3/g.

Table 5 presents the yields obtained during each stage of the process and the overall yield. The overall yield decreased considerably with

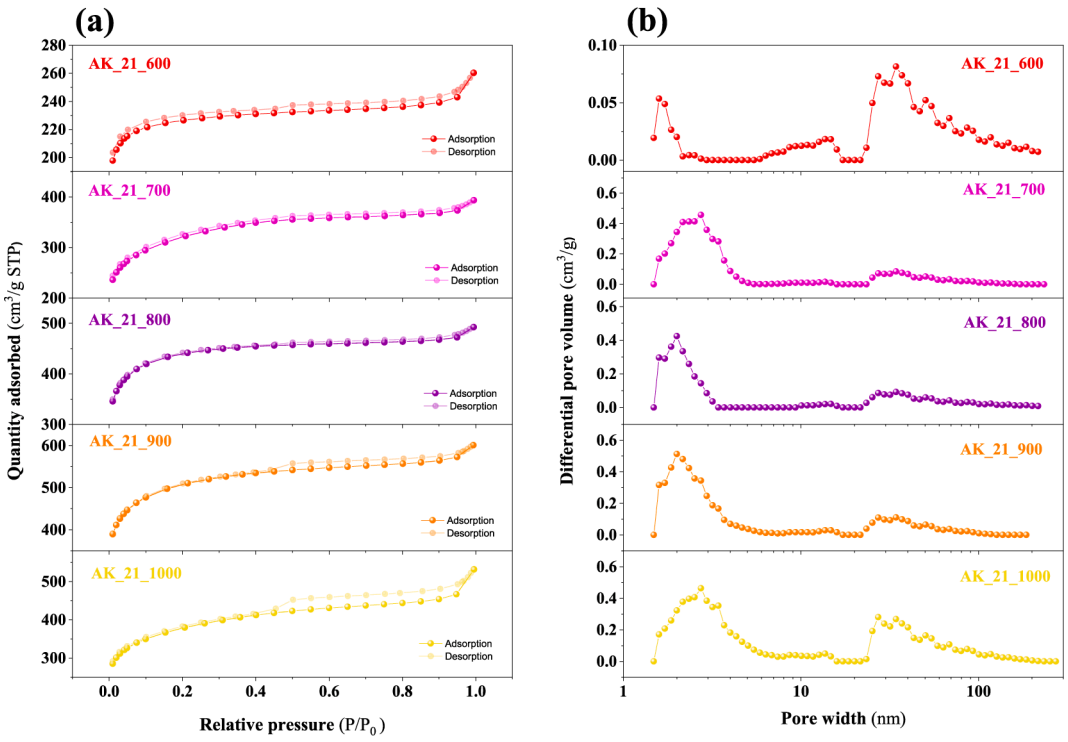

Fig. 3. **(a)** N_2 adsorption/desorption isotherms and **(b)** pore size distributions for ACs prepared at different pyrolysis temperatures.

Table 5
Yields of the process for ACs prepared at a 2:1 mass ratio and different pyrolysis temperatures.

Samples	*Thermochemical treatment yield*	*Chemical purification yield*	*Overall yield*
	(%)	*(%)*	*(%)*
AK_21_600	50.19	22.51	11.30
AK_21_700	48.91	19.38	9.38
AK_21_800	47.59	19.55	9.31
AK_21_900	37.72	14.23	5.37
AK_21_1000	21.17	10.38	2.29

The standard deviation between replicates was less than 0.01 % in all cases.

increasing temperatures. This may have occurred because the thermochemical treatment and chemical purification yield also decreased by 58 % and 80 %, respectively. The TGA under nitrogen atmosphere (Fig. 1) demonstrated that as the temperature increased, a progressive weight reduction continued. This is consistent with the fact that the thermochemical treatment yield decreased as the temperature increased. It should be noted that the overall yield values are higher than those reported for the synthesis of other biomass-derived ACs (also obtained by direct activation with KOH at similar temperatures)[54], even when the weight of the activating agent in the present study is considered in this calculation.

After analysing all the results, the AC that exhibited better physicochemical and textural characteristics although not the best yields was the sample with 2:1 A:K mass ratio pyrolysed at 900 °C (AK_21_900). This AC was selected because its adequate physico-chemical characteristics and optimal textual properties could make it an excellent material for applications with higher added value.

In these applications, the role of functional groups is very important. To investigate this, an FT-IR spectrum of the AK_21_900 sample was conducted, as shown in Fig. S4. The different bands were assigned based on previous literature on EOP-derived ACs [8,26]. The spectrum of the sample exhibited a relatively simple pattern characterised by four main bands: firstly, a strong band centred at 3460 cm −1 corresponded to the O–H stretching vibration; secondly, the peak at 1640 cm −1 was attributed to aromatic C = C stretching vibrations, which overlapped with the peaks corresponding to the C = O bond stretching vibrations; thirdly, the band observed at 1384 cm −1 was assigned to C–H deformation vibration; and finally, the one centred at 1050 cm −1 corresponded to C–C and C–O single bonds. Additionally, to determine the surface charge exhibited by the ACs for future applications as adsorbents, zeta potential measurements were conducted, as represented in Fig. S5. As shown in the graph, the external surface charge of the AC decreased as the pH increased, indicating a shift towards a more negative charge. The isoelectric point was reached at highly acidic pH values (pH ≈ 2). These results are consistent with previous studies on the zeta potential conducted on various biomass-derived ACs [31,42,61]. The outcomes confirm the suitability of this material for its application as an adsorbent for cationic contaminants, such as metals in wastewater.

Therefore, the combination of high carbon content, high specific surface area, the presence of functional groups, and the external negative surface charge are key properties of the ACs for their effective utilisation in catalysis, adsorption, and energy storage applications [18]. For instance, Jawad et al. [34] studied the adsorption capacity of a high surface area AC obtained from dragon fruit peels and confirmed its effectiveness due to its textural properties. Similarly, Lee et al. [36] demonstrated that ACs specifically derived from coconut shells that exhibit a high surface area present superior electrochemical performance for their application in supercapacitors.

3.4. Evaluation of the gaseous and liquid streams generated during the process to transform alpeorujo into AC

Finally, the gaseous emissions generated during the pyrolytic process were characterised to determine their composition and concentration. In addition, the chemical purification liquids and wash water were also analysed in order to evaluate the possibility of reusing both. These characterisations were performed on a sample with an A:K ratio of 2:1 calcined at 900 °C (AK_21_900).

3.4.1. Analysis of the condensable and non-condensable fractions generated during thermochemical treatment

The non-condensable gases generated throughout the pyrolytic process were characterised by GC/MS, allowing the identification of a wide variety of compounds. As can be observed in Table S1, there is a predominance of aliphatic hydrocarbon families, with a notable presence of cyclopropane and pentane at concentrations of 6.66 and 2.77 mg/g of *alpeorujo*, respectively. These compounds are of great relevance since they can be used as fuels [52]. Fig. S6 shows the chromatogram obtained from the thermochemical treatment performed on the AK_21_900 sample.

The total production of VOCs and VSCs, expressed as $mg/kg_{Alpeorujo}$, was calculated by the continuous mass balance of the non-stationary process to the non-condensable gases. The results showed a total yield of 874 $mg_{VOC}/kg_{Alpeorujo}$ and 2605 $mg_{VSC}/kg_{Alpeorujo}$, with 75 % being sulphur-based compounds.

Fig. 4a shows the variation in the yield of the gaseous emission of VOCs ($mg_{VOC}/kg_{Alpeorujo}$) and VSCs ($mg_{VSC}/kg_{Alpeorujo}$) quantified at different times of the pyrolytic process, as explained in the Materials and Methods section.

As shown in Fig. 4a, VSC emission began at 300 °C and reached a maximum concentration of 50 $mg_{VSC}/kg_{Alpeorujo}$. Subsequently, this emission decreased to 10 $mg_{VSC}/kg_{Alpeorujo}$ and was maintained at this level until the end of the experiment. The spectrum of VSC shown in Fig. 4b demonstrates the major generation of dimethyl sulphide (DMS) and H_2S. Likewise, methyl-SH, DMDS, and ethyl-SH gases were identified with yields below 5 $mg/kg_{Alpeorujo}$. The concentration of VOCs increased slightly with temperatures up to 500 °C, where it remained constant at about 7 $mg_{VOC}/kg_{Alpeorujo}$ until the end of the experiment. This indicated that the rest of the gaseous organic compounds generated during the thermochemical treatment were condensed when passing through the cold chamber (pyrolysis distillates).

This dry, condensed fraction, called distillate, was also characterised. Firstly, the molecular formula of pyrolysis distillates was determined by elemental analysis, which was $C_{63}H_{39}N_{12}SO_{26}$. To determine the energy capacity of this fraction, its HHV was measured by means of a calorimeter, which allowed us to calculate the lower heating value (LHV), which was 13810 kcal/kg. From this value, an energy yield of 13810 kcal/t of *alpeorujo* was determined. Finally, the main compounds present in the condensed fraction were identified by GC/MS. Phenolic derivatives were the main compounds identified (approximately 75 %) along with other important compounds (2,4-dimethylfuran, 2-methyl-2-cyclopentane, 3-dimethylamine, etc.). Based on these results, pyrolysis distillates represent a very interesting fraction because they can be a source of carbon that can be recovered in the form of fuel.

3.4.2. Study of liquid effluents generated during the purification and washing stages

The elements present in the AC after both stages, calculated by Eqs. (5) and (6), are shown in Table 6. The results of the percentage of elements removed from the *alpeorujo*, as calculated by Eq. (7), are also shown.

The number of elements originally present in the *alpeorujo*, listed in Table 1, were almost completely eliminated with these treatments, with some exceptions. In the case of Fe and Ni, they were not completely eliminated since they remain in the oxide form in the AC. As regards S, a material balance demonstrated that part of it was removed in the form of VSC in the gaseous effluent. This will be demonstrated subsequently in this investigation by eliminating another fraction in thermochemical treatment distillates. This did not imply that the AC obtained had a high sulphur concentration.

These were not the only elements removed during the chemical purification and washing process. KOH was added as an activating agent in the mechanical pre-activation stage and transformed into potassium oxide during the thermochemical treatment process. Moreover, the addition of HCl during the chemical purification stage increased the concentration of chloride quantified in the material balance. Because these two elements were not derived entirely from the raw material they are not included in Table 6.

The removal of the abovementioned elements in the ACs from *alpeorujo* after the chemical purification and washing stages was confirmed through SEM/EDS mapping, which verified that some of them were no longer detected (Fig. S6). Based on these results, it can be confirmed that the chemical purification and washing processes were very efficient. The composition of this liquid stream suggests the potential for reuse in the same process as long as it maintains its acidic character and continues to extract metals from ACs efficiently [49].

A physicochemical characterisation of the washing effluents was also conducted and the results are shown in Table S2. The effluents had very high conductivity values and low pH (3340 μS/cm and 1.94, respectively). It is important to note that concentration of chlorides exceeded 2000 mg/L, which could have a significant environmental impact in

Table 6
Content of recovered elements during the chemical purification and washing stages.

Element	*Chemical purification (mg/g AC)*	*Washing (mg/g AC)*	*Total (mg/g AC)*	*Elements removed regarding to alpeorujo (%)*
P	14.87	16.27	31.13	97.99
Ca	87.60	27.57	115.17	98.30
Mg	25.87	12.88	38.75	99.05
S	4.14	7.03	11.17	49.72
Al	7.59	6.57	14.16	99.82
Fe	4.78	0.00	4.78	61.70
Na	1.77	0.76	2.53	97.78
Ni	0.04	0.23	0.28	66.33

The standard deviation between replicates was less than 0.01 % in all cases.

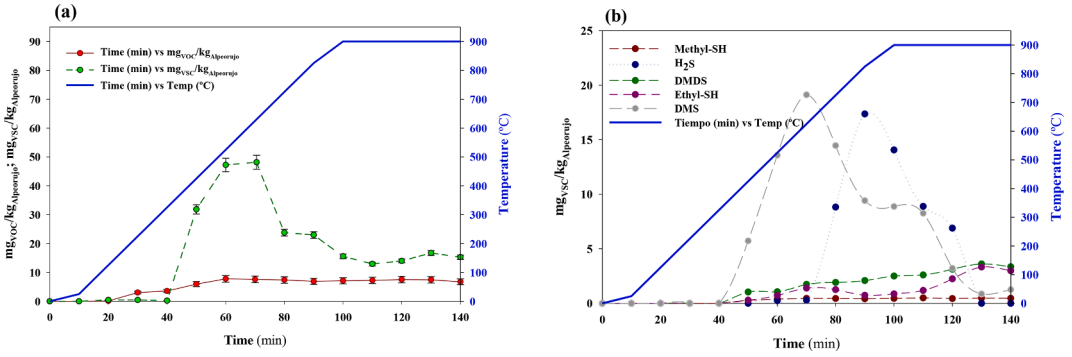

Fig. 4. **(a)** Evolution of VOC and VSC generation and **(b)** breakdown in the evolution of VSC generation during the thermochemical treatment process of the AK_21_900 sample.

some natural areas. Note that the highest proportion of solids present in the waters corresponded to the mineral fraction (80 %), so there was not a high amount of organic pollution and its values were suitable for discharge [20].

3.5. Economic and energy balance

A preliminary economic and energy balance was carried out considering experimental conditions at laboratory scale. Specifically, the energy consumption of the *alpeorujo* drying stage and subsequent pyrolytic process (oven and flowmeter) were considered. The cost of the nitrogen flow used in the thermochemical treatment to carry out the process under inert conditions and the cost of the activating agent used were also included. The initial hypothesis included the following prices: average unit price in 2022 of company electricity = €0.174/kWh (Statistical Office of the European Communities, Eurostat), the unit price of N_2 gas for major consumers = €0.5/m^3, and industrial price of potassium hydroxide = €800/t. The cost of the raw material was considered to be zero because it is a residue. At the laboratory level, the furnace and flow meter output were 2500 W and 2.00 W, respectively.

To determine the energy balance of drying the raw material, first, the total energy required to remove the water from 1 ton of wet *alpeorujo* was calculated, taking into account that it had 70 % moisture. This value corresponded to 2613 MJ/t water, which translated into 1829 MJ/t of wet *alpeorujo*, where 86 % refers to the evaporative energy and the remaining 14 % to sensitive heat when drying at a temperature in the range of 20–105 °C.

Once the energy balance of the drying stage was achieved, the energy balance during the thermochemical treatment stage was estimated. An initial mass of 1 t of wet *alpeorujo* was selected, which leads to 0.45 t of the initial mixture, maintaining the 2:1 ratio between dry *alpeorujo* and activating agent (KOH). It was determined that the total energy consumed during the pyrolytic process by the furnace and the flowmeter was 7942 MJ per t wet *alpeorujo*. Once the energy requirement during drying and thermochemical treatment was known, it could be determined that the total energy consumed in the transformation of *alpeorujo* into AC was 9771 MJ/t of wet *alpeorujo*. Of this, 81 % corresponds to the energy used during the pyrolytic process and the remaining 19 % corresponds to the drying stage.

Finally, an economic balance was made based on the previously mentioned operating costs. Cost analysis is very important in determining the viability of the AC production process. The final price of the treatment was €0.21/kg for the wet process, with a total production price of €9.28 for one kilogram of AC generated. This value is consistent with previous studies that have estimated the cost of AC production at 233.81 INR (Indian Rupee), taking into account that the price difference was due to the fact that the cost of electricity in other countries is almost four times lower than in Europe [15].

For a more extensive economic study, a sensitivity analysis was conducted to understand how variations in different parameters and experimental conditions might impact the final product price. Firstly, it is important to mention that varying the ratio of *alpeorujo* and KOH to 1:1 and 3:1 resulted in an increase of 19 % and a decrease of 12 % in the final price, respectively, in relation to the *alperujo*:KOH ratio selected as a reference for the economic study (2:1).

Variations in price due to changes in the conditions and variables that offer the best structural properties in the final product is shown in Table 7. As can be observed, the variable that most affects the final cost is the initial moisture content of the *alpeorujo* is the variable that has the greatest impact on the final cost. When this percentage varied between 7 and 28 %, the final price of the product was significantly affected and increased by up to 120 %. This variation is non-linear with respect to the cost. As regards the variation in the price of KOH, given the high volatility of prices, no significant effect on the final price was observed (between 1.4–3.6 %). Furthermore, the ratio 2:1 resulted in a small amount of KOH, which further minimised the effect on the final product price. Another variable that did not significantly affect the final price was the pyrolysis temperature, as the thermochemical treatment was carried out on previously dried material. The variation in final temperature did not affect the cost as much as the experimentation time. However, a variation in the price of electricity resulted in a proportional variation in the final price of between 2.5 and 6.5 %.

Table 7
Sensitivity analysis results.

	Range of variable variation (%)	*Variation in the final product cost (%)*
Moisture of the alpeorujo	7–28	12–120
KOH price	2.5–25	1.4–3.6
Pyrolisis temperature	5–50	< 2
Electricity price	6–15	2.5–6.5

4. Conclusions

Alpeorujo was demonstrated to be a valuable waste with a high organic matter content. It is suitable for obtaining highly porous ACs by a simple thermochemical process using low-ratio KOH as an activating agent and temperatures close to 900 °C. A total yield of VSCs that was three times higher than VOCs was quantified in the gaseous streams of the thermochemical treatment, thus suggesting the need for a future assessment of control systems for these emissions. Almost 100 % of the elements present in the *alpeorujo* were removed by chemical purification, generating potentially reusable and valorisable liquid effluents. Although the pyrolytic process corresponds to 80 % of the energy consumption, the simple production process allowed obtaining an AC cost below €9.30/kg. Given the physicochemical characteristics, textural properties, and cost-effectiveness of the *alpeorujo*-derived AC, its potential application as a catalyst, adsorbent, and for energy storage is proposed for future investigations.

CRediT authorship contribution statement

H. Martínez-Alvarenga: Writing – original draft, Visualization, Validation, Software, Methodology, Investigation, Formal analysis, Conceptualization. **M.C. Gutiérrez:** Writing – original draft, Visualization, Validation, Software, Methodology, Investigation, Formal analysis, Conceptualization. **A. Benítez:** Writing – original draft, Visualization, Validation, Software, Methodology, Investigation, Funding acquisition, Formal analysis, Conceptualization. **M.A. Martín:** Validation, Supervision, Resources, Project administration, Methodology, Funding acquisition, Formal analysis, Data curation, Conceptualization. **A. Caballero:** Writing – original draft, Visualization, Validation, Software, Methodology, Investigation, Funding acquisition, Formal analysis, Conceptualization.

Declaration of competing interest

The authors declare that they have no known competing financial interests or personal relationships that could have appeared to influence the work reported in this paper.

Data availability

Data will be made available on request.

Acknowledgments

This research has been funded by the Campus de Excelencia Internacional Agroalimentario (Project OLIVE2ENERGY PYC20 RE 048 UCO); Cordoba University (Plan Propio de Investigación 2023,

UCOLIDERA); Ministerio de Ciencia e Innovación MCIN/AEI/10.13039/501100011033 (Projects PID2020-117438RB-I00 & PID2020-113931RB-I00), European Union "NextGenerationEU"/PRTR (Projects PDC2021-120903-I00 & TED2021-130668B-I00; and Juan de la Cierva – Incorporación fellowship IJC2020-045041-I); Junta de Andalucía (Project GOPO-CO-23-0006, Grupos Operativos de la Asociación Europea de Innovación -AEI-). The authors wish to acknowledge the technical staff from the Instituto Químico para la Energía y el Medioambiente (IQUEMA), Servicio Central de Apoyo a la Investigación (SCAI) of Cordoba University and express special gratitude to Inmaculada Bellido and Rafael Pérez for their contribution to this research. Funding for open access charge: University of Córdoba/CBUA.

Appendix A. Supplementary material

Supplementary material to this article can be found online at https://doi.org/10.1016/j.fuel.2024.132502.

References

[1] Abid N, Masmoudi MA, Megdiche M, Barakat A, Ellouze M, Chamkha M, et al. Biochar from olive mill solid waste as an eco-friendly adsorbent for the removal of polyphenols from olive mill wastewater. Chem Eng Res Des 2022;181:384–98. https://doi.org/10.1016/j.cherd.2022.02.029.

[2] Abu-Dalo M, Abdelnabi J, Bawab A Al. Preparation of activated carbon derived from jordanian olive cake and functionalized with Cu/Cu_2O/CuO for adsorption of phenolic compounds from olive mill wastewater. Materials 2021;14(6636). https://doi.org/10.3390/MA14216636.

[3] Aguilera E, Guzmán G, Alonso A. Greenhouse gas emissions from conventional and organic cropping systems in Spain I Herbaceous crops. Agron Sustain Dev 2015;35:713–24. https://doi.org/10.1007/s13593-014-0267-9.

[4] Ai W, Zhou W, Du Z, Chen Y, Sun Z, Wu C, et al. Nitrogen and phosphorus codoped hierarchically porous carbon as an efficient sulfur host for Li-S batteries. Energy Storage Mater 2017;6:112–8. https://doi.org/10.1016/J.ENSM.2016.10.008.

[5] Alburquerque JA, Gonzálvez J, Tortosa G, Baddi GA, Cegarra J. Evaluation of "alperujo" composting based on organic matter degradation, humification and compost quality. Biodegradation 2009;20:257–70. https://doi.org/10.1007/s10532-008-9218-y.

[6] Angin D, Altintig E, Köse TE. Influence of process parameters on the surface and chemical properties of activated carbon obtained from biochar by chemical activation. Bioresour Technol 2013;148:542–9. https://doi.org/10.1016/J.BIORTECH.2013.08.164.

[7] APHA, American Public Health Association, American Water Works Association, Water Environment Federation, 2023. Methods for the Examination of Water and Wastewater. 24th ed. https://www.standardmethods.org/24theditioncitation (accessed 9.7.23).

[8] Awad, S., Villot, A., Abderrabba, M., Tazerout, M., 2020. Heterogeneous Acid Catalyst Preparation from Olive Pomace and its Use for Olive Pomace Oil Esterification 2 Manel AYADI a.

[9] Ayadi M, Awad S, Villot A, Abderrabba M, Tazerout M. Heterogeneous acid catalyst preparation from olive pomace and its use for olive pomace oil esterification. Renew Energy 2021;165(2):1–13. https://doi.org/10.1016/j.renene.2020.11.031.

[10] Batuecas E, Tommasi T, Battista F, Negro V, Sonetti G, Viotti P, et al. Life Cycle Assessment of waste disposal from olive oil production: anaerobic digestion and conventional disposal on soil. J Environ Manage 2019;237:94–102. https://doi.org/10.1016/j.jenvman.2019.02.021.

[11] Borja R, Martín A, Alonso V, García I, Banks CJ. Influence of different aerobic pretreatments on the kinetics of anaerobic digestion of olive mill wastewater. Water Res 1995;29:489–95. https://doi.org/10.1016/0043-1354(94)00180-F.

[12] Caputo MC, De Girolamo AM, Volpe A. Soil amendment with olive mill wastes: impact on groundwater. J Environ Manage 2013;131:216–21. https://doi.org/10.1016/j.jenvman.2013.10.004.

[13] Carmona I, Aguirre I, Griffith DM, García-Borrego A. Towards a circular economy in virgin olive oil production: Valorization of the olive mill waste (OMW) "alpeorujo" through polyphenol recovery with natural deep eutectic solvents (NADESs) and vermicomposting. Sci Total Environ 2023;872:162198. https://doi.org/10.1016/J.SCITOTENV.2023.162198.

[14] Cervilla LM, Blasco B, Rios JJ, Rosales MA, Sánchez-Rodríguez E, Rubio-Wilhelmi MM, et al. Parameters symptomatic for boron toxicity in leaves of tomato plants. J Bot 2012;2012:1–17. https://doi.org/10.1155/2012/726206.

[15] Chauhan PR, Raveesh G, Pal K, Goyal R, Tyagi SK. Production of biomass derived highly porous activated carbon: a solution towards in-situ burning of crop residues in India. Bioresour Technol Rep 2023;22:101425. https://doi.org/10.1016/J.BITEB.2023.101425.

[16] Chayid MA, Ahmed MJ. Amoxicillin adsorption on microwave prepared activated carbon from Arundo donax Linn: Isotherms, kinetics, and thermodynamics studies. J Environ Chem Eng 2015;3:1592–601. https://doi.org/10.1016/J.JECE.2015.05.021.

[17] Chen Y, Zhang X, Chen W, Yang H, Chen H. The structure evolution of biochar from biomass pyrolysis and its correlation with gas pollutant adsorption performance. Bioresour Technol 2017;246:101–9. https://doi.org/10.1016/J.BIORTECH.2017.08.138.

[18] Chen Y, Zhu Y, Wang Z, Li Y, Wang L, Ding L, et al. Application studies of activated carbon derived from rice husks produced by chemical-thermal process—a review. Adv Colloid Interface Sci 2011;163:39–52. https://doi.org/10.1016/J.CIS.2011.01.006.

[19] Deiana AC, Sardella MF, Silva H, Amaya A, Tancredi N. Use of grape stalk, a waste of the viticulture industry, to obtain activated carbon. J Hazard Mater 2009;172:13–9. https://doi.org/10.1016/J.JHAZMAT.2009.06.095.

[20] Directive 91/271/CEE, of 21 May 1991, on the treatment of urban wastewater. Official Journal of the European Union, L135, 30 May 1991.

[21] Duan C, Meng M, Huang H, Wang H, Zhang Q, Gan W, et al. Performance and characterization of bamboo-based activated carbon prepared by boric acid activation. Mater Chem Phys 2023;295:127130. https://doi.org/10.1016/J.MATCHEMPHYS.2022.127130.

[22] El-Bassi L, Azzaz AA, Jellali S, Akrout H, Marks EAN, Ghimbeu CM, et al. Application of olive mill waste-based biochars in agriculture: Impact on soil properties, enzymatic activities and tomato growth. Sci Total Environ 2021;755. https://doi.org/10.1016/j.scitotenv.2020.142531.

[23] El-Hendawy ANA. An insight into the KOH activation mechanism through the production of microporous activated carbon for the removal of Pb^{2+} cations. Appl Surf Sci 2009;255:3723–30. https://doi.org/10.1016/J.APSUSC.2008.10.034.

[24] Ello AS, De Souza LKC, Trokourey A, Jaroniec M. Development of microporous carbons for CO_2 capture by KOH activation of African palm shells. J CO_2 Util 2013;2:35–8. https://doi.org/10.1016/J.JCOU.2013.07.003.

[25] Elmouwahidi A, Bailón-García E, Pérez-Cadenas AF, Maldonado-Hódar FJ, Carrasco-Marín F. Activated carbons from KOH and H3PO4-activation of olive residues and its application as supercapacitor electrodes. Electrochim Acta 2017;229:219–28. https://doi.org/10.1016/J.ELECTACTA.2017.01.152.

[26] Elmouwahidi A, Vivo-Vilches JF, Pérez-Cadenas AF, Maldonado-Hódar FJ, Carrasco-Marín F. Free metal oxygen-reduction electro-catalysts obtained from biomass residue of the olive oil industry. Chem Eng J 2016;306:1109–15. https://doi.org/10.1016/j.cej.2016.08.042.

[27] Fernández-Lobato L, López-Sánchez Y, Blejman G, Jurado F, Moyano-Fuentes J, Vera D. Life cycle assessment of the Spanish virgin olive oil production: A case study for Andalusian region. J Clean Prod 2021;290. https://doi.org/10.1016/j.jclepro.2020.125677.

[28] García-Mateos FJ, Ruiz-Rosas R, Marqués MD, Cotoruelo LM, Rodríguez-Mirasol J, Cordero T. Removal of paracetamol on biomass-derived activated carbon: modeling the fixed bed breakthrough curves using batch adsorption experiments. Chem Eng J 2015;279:18–30. https://doi.org/10.1016/j.cej.2015.04.144.

[29] Gayathiri M, Pulingam T, Lee KT, Sudesh K. Activated carbon from biomass waste precursors: factors affecting production and adsorption mechanism. Chemosphere 2022. https://doi.org/10.1016/j.chemosphere.2022.133764.

[30] Gómez-Cruz I, del Mar Contreras M, Romero I, Castro E. A biorefinery approach to obtain antioxidants, lignin and sugars from exhausted olive pomace. J Ind Eng Chem 2021;96:356–63. https://doi.org/10.1016/j.jiec.2021.01.042.

[31] Han Q, Wang J, Goodman BA, Xie J, Liu Z. High adsorption of methylene blue by activated carbon prepared from phosphoric acid treated eucalyptus residue. Powder Technol 2020;366:239–48. https://doi.org/10.1016/J.POWTEC.2020.02.013.

[32] Heidarinejad Z, Dehghani MH, Heidari M, Javedan G, Ali I, Sillanpää M. Methods for preparation and activation of activated carbon: a review. Environ Chem Lett 2020;18(2):393–415. https://doi.org/10.1007/S10311-019-00955-0.

[33] Hussain OA, Hathout AS, Abdel-Mobdy YE, Rashed MM, Abdel Rahim EA, Fouzy ASM. Preparation and characterization of activated carbon from agricultural wastes and their ability to remove chlorpyrifos from water. Toxicol Rep 2023;10:146–54. https://doi.org/10.1016/J.TOXREP.2023.01.011.

[34] Jawad AH, Saud Abdulhameed A, Wilson LD, Syed-Hassan SSA, ALOthman ZA, Rizwan Khan M. High surface area and mesoporous activated carbon from KOH-activated dragon fruit peels for methylene blue dye adsorption: optimization and mechanism study. Chin J Chem Eng 2021;32:281–90. https://doi.org/10.1016/J.CJCHE.2020.09.070.

[35] Lee HM, An KH, Kim BJ. Effects of carbonization temperature on pore development in polyacrylonitrile-based activated carbon nanofibers. Carbon Lett 2014;15:146–50. https://doi.org/10.5714/CL.2014.15.2.146.

[36] Lee KC, Lim MSW, Hong ZY, Chong S, Tiong TJ, Pan GT, Huang CM. Coconut shell-derived activated carbon for high-performance solid-state supercapacitors. Energies 2021;14:4546. https://doi.org/10.3390/EN14154546.

[37] Li B, Dai F, Xiao Q, Yang L, Shen J, Zhang C, et al. Nitrogen-doped activated carbon for a high energy hybrid supercapacitor. Energy Environ Sci 2016;9:102–6. https://doi.org/10.1039/C5EE03149D.

[38] López-Cano I, Roig A, Cayuela ML, Alburquerque JA, Sánchez-Monedero MA. Biochar improves N cycling during composting of olive mill wastes and sheep manure. Waste Manag 2016;49:553–9. https://doi.org/10.1016/j.wasman.2015.12.031.

[39] Lua AC, Yang T. Effect of activation temperature on the textural and chemical properties of potassium hydroxide activated carbon prepared from pistachio-nut shell. J Colloid Interf Sci 2004;274:594–601. https://doi.org/10.1016/J.JCIS.2003.10.001.

[40] Márquez P, Gutiérrez MC, Toledo M, Alhama J, Michán C, Martín MA. Activated sludge process versus rotating biological contactors in WWTPs: evaluating the influence of operation and sludge bacterial content on their odor impact. Process Saf Environ Prot 2022;160:775–85. https://doi.org/10.1016/j.psep.2022.02.071.

[41] Michailides M, Christou G, Akratos CS, Tekerlekopoulou AG, Vayenas DV. Composting of olive leaves and pomace from a three-phase olive mill plant. Int

Biodeterior Biodegradation 2011;65:560–4. https://doi.org/10.1016/j.ibiod.2011.02.007.
[42] Mozhiarasi V, Natarajan TS. Bael fruit shell–derived activated carbon adsorbent: effect of surface charge of activated carbon and type of pollutants for improved adsorption capacity. Biomass Convers Biorefin 2022;14:8761–74. https://doi.org/10.1007/S13399-022-03211-8/FIGURES/14.
[43] Orive M, Cebrián M, Amayra J, Zufía J, Bald C. Integrated biorefinery process for olive pomace valorisation. Biomass Bioenergy 2021;149. https://doi.org/10.1016/j.biombioe.2021.106079.
[44] Paz A, Karnaouri A, Templis CC, Papayannakos N, Topakas E. Valorization of exhausted olive pomace for the production of omega-3 fatty acids by crypthecodinium cohnii. Waste Manag 2020;118:435–44. https://doi.org/10.1016/j.wasman.2020.09.011.
[45] Rajendran N, Gurunathan B, Han J, Krishna S, Ananth A, Venugopal K, et al. Recent advances in valorization of organic municipal waste into energy using biorefinery approach, environment and economic analysis. Bioresour Technol 2021. https://doi.org/10.1016/j.biortech.2021.125498.
[46] Rincón B, Rodríguez-Gutiérrez G, Bujalance L, Fernández-Bolaños J, Borja R. Influence of a steam-explosion pre-treatment on the methane yield and kinetics of anaerobic digestion of two-phase olive mil solid waste or alperujo. Process Saf Environ Prot 2016;102:361–9. https://doi.org/10.1016/j.psep.2016.04.010.
[47] Roselló-Soto E, Koubaa M, Moubarik A, Lopes RP, Saraiva JA, Boussetta N, et al. Emerging opportunities for the effective valorization of wastes and by-products generated during olive oil production process: Non-conventional methods for the recovery of high-added value compounds. Trends Food Sci Technol 2015. https://doi.org/10.1016/j.tifs.2015.07.003.
[48] Roulia M, Kontezaki E, Kalogeropoulos N, Chassapis K. One step bioremediation of olive-oil-mill waste by organoinorganic catalyst for humics-rich soil conditioner production. Agronomy 2021;11:1114. https://doi.org/10.3390/AGRONOMY11061114/S1.
[49] Shyam Sunder GS, Adhikari S, Rohanifar A, Poudel A, Kirchhoff JR. Evolution of environmentally friendly strategies for metal extraction. Separations 2020;7. https://doi.org/10.3390/SEPARATIONS7010004.
[50] Şirazi M, Aslan S. Comprehensive characterization of high surface area activated carbon prepared from olive pomace by KOH activation. Chem Eng Commun 2021;208:1479–93. https://doi.org/10.1080/00986445.2020.1864628.
[51] Sreńscek-Nazzal J, Kamińska A, Serafin J, Michalkiewicz B. Chemical activation of banana peel waste-derived biochar using KOH and urea for CO_2 Capture. Materials 2024;17:872. https://doi.org/10.3390/MA17040872.
[52] Su X, Zhang F, Yin Y, Tu B, Cheng M. Thermodynamic analysis and fuel processing strategies for propane-fueled solid oxide fuel cell. Energy Convers Manag 2020;204:112279. https://doi.org/10.1016/J.ENCONMAN.2019.112279.
[53] Suhas CPJM, Ribeiro Carrott MML. Lignin - from natural adsorbent to activated carbon: A review. Bioresour Technol 2007;98:2301–12. https://doi.org/10.1016/j.biortech.2006.08.008.
[54] Tay T, Ucar S, Karagöz S. Preparation and characterization of activated carbon from waste biomass. J Hazard Mater 2009;165:481–5. https://doi.org/10.1016/J.JHAZMAT.2008.10.011.
[55] TMECC, Test Methods for the Examination of Compost and Composting, 2002. US Composting Council. https://www.compostingcouncil.org/page/tmecc (accessed 7.17.23).
[56] Toledo M, Gutiérrez MC, Peña A, Siles JA, Martín MA. Co-composting of chicken manure, alperujo, olive leaves/pruning and cereal straw at full-scale: compost quality assessment and odour emission. Process Saf Environ Prot 2020;139:362–70. https://doi.org/10.1016/j.psep.2020.04.048.
[57] Tortosa G, Alburquerque JA, Ait-Baddi G, Cegarra J. The production of commercial organic amendments and fertilisers by composting of two-phase olive mill waste ("alperujo"). J Clean Prod 2012;26:48–55. https://doi.org/10.1016/J.JCLEPRO.2011.12.008.
[58] Varnero MT, Galleguillos K, Guerrero D, Suárez J. Producción de Biogás y enmiendas orgánicas a partir del residuo olivícola (Alperujo). Información Tecnológica 2014;25:73–8. https://doi.org/10.4067/S0718-07642014000500011.
[59] Wang Y, Wang ling S, Xie T, Cao J. Activated carbon derived from waste tangerine seed for the high-performance adsorption of carbamate pesticides from water and plant. Bioresour Technol 2020;316. https://doi.org/10.1016/j.biortech.2020.123929.
[60] Wu FC, Wu PH, Tseng RL, Juang RS. Preparation of activated carbons from unburnt coal in bottom ash with KOH activation for liquid-phase adsorption. J Environ Manage 2010;91:1097–102. https://doi.org/10.1016/J.JENVMAN.2009.12.011.
[61] Zubrik A, Matik M, Hredzák S, Lovás M, Danková Z, Kováčová M, et al. Preparation of chemically activated carbon from waste biomass by single-stage and two-stage pyrolysis. J Clean Prod 2017;143:643–53. https://doi.org/10.1016/J.JCLEPRO.2016.12.061.